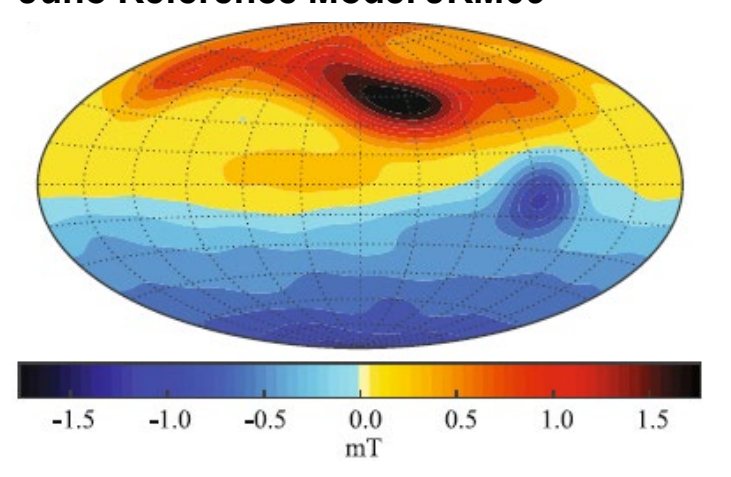
International Conference on Strongly Coupled Coulomb Systems (SCCS), Stateline/NV, 27 July – 1 August 2025

A conductivity model based on ab initio simulations

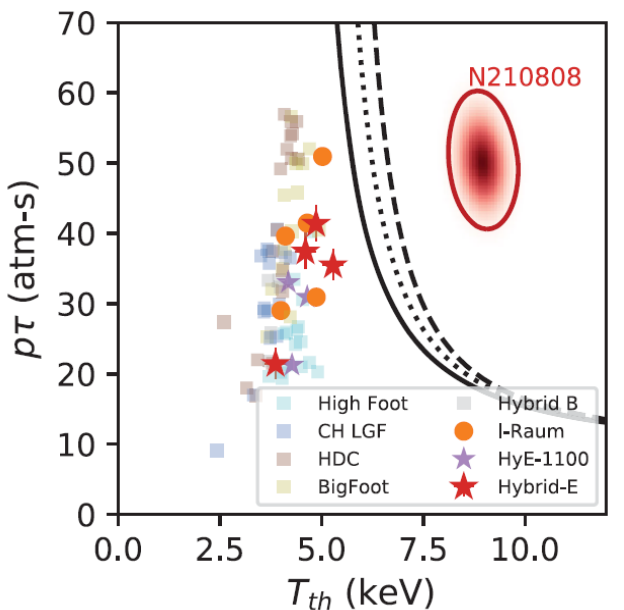
Uwe Kleinschmidt and Ronald Redmer

University of Rostock, Institute of Physics, 18051 Rostock, Germany

Juno Reference Model JRM09



J. Wicht & U.R. Christensen, JGR Planets **129**, e2023JE007890 (2024)



Breakthrough at the NIF on Dec 5, 2022: Ignition reached using laser indirect drive,

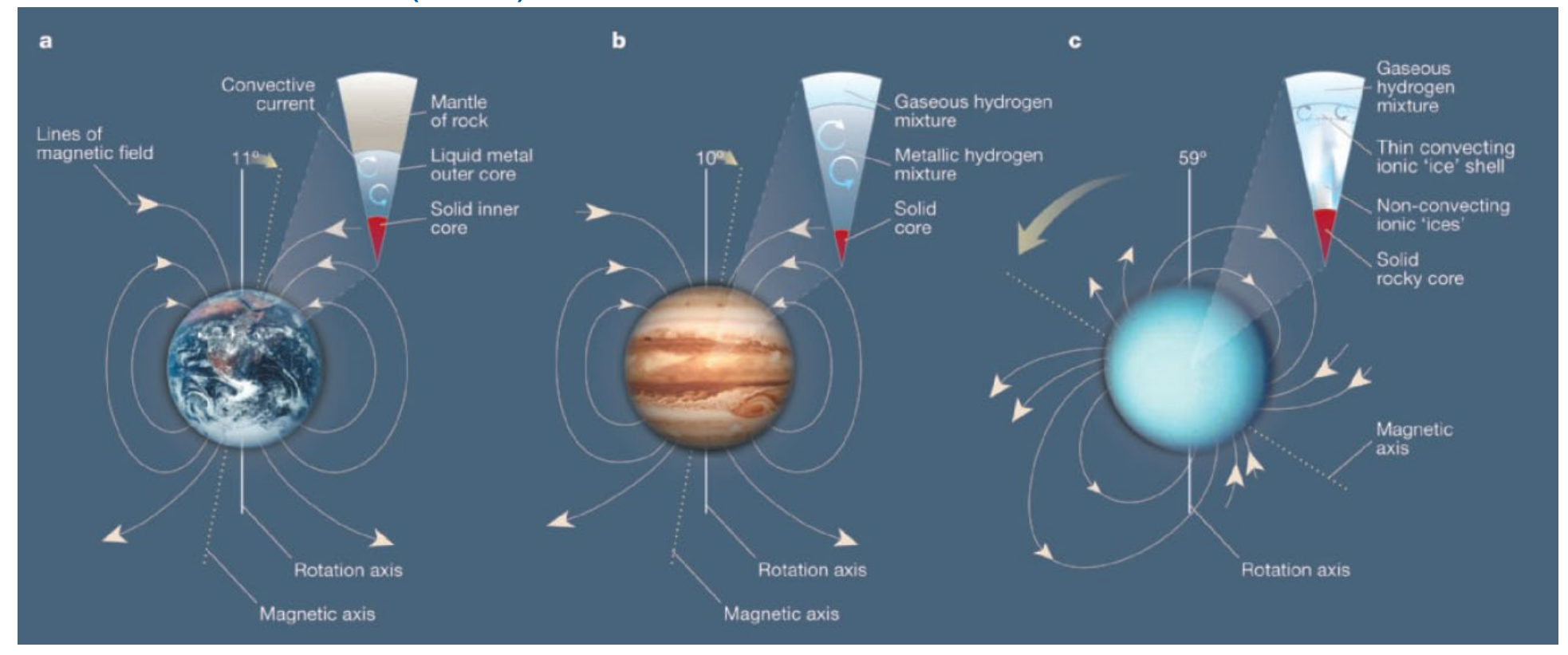
see H. Abu-Shawared et al.

Phys. Rev. Lett. 129, 075001 (2022)

Phys. Rev. Lett, **132**, 065102 (2024)

Interior and magnetic field of solar system planets

J. Aurnou, Nature **428**, 134 (2004)



Dynamo simulations solve magneto-hydrodynamic equations for planetary interiors; see e.g.

Stanley & Bloxham 2004, 2006, Wicht & Tilgner 2010, Christensen 2010, Stanley & Glatzmaier 2010, Tian & Stanley 2013, Jones 2014, Gastine et al. 2014, Connerny et al. 2021, Wicht & Christensen 2024 ...

Accurate EOS and transport data are needed: profiles for P(r), $\rho(r)$, T(r) and $\sigma(r)$, $\lambda(r)$, $\eta(r)$...



The famous Spitzer theory for fully ionized plasmas

L. Spitzer Jr. & R. Härm, Phys. Rev. 89, 977 (1953), more than 2000 citations

Exact analytical results for the transport coefficients in the low-density, high-temperature limit based on a solution of the Fokker-Planck kinetic equation. Valid for arbitrary ion charge Z and accounting for electron-electron scattering.

PHYSICAL REVIEW

VOLUME 89, NUMBER 5

MARCH 1, 1953

Transport Phenomena in a Completely Ionized Gas*

Lyman Spitzer, Jr., and Richard Härm Princeton University Observatory, Princeton, New Jersey (Received November 10, 1952)

The coefficients of electrical and thermal conductivity have been computed for completely ionized gases with a wide variety of mean ionic charges. The effect of mutual electron encounters is considered as a problem of diffusion in velocity space, taking into account a term which previously had been neglected. The appropriate integro-differential equations are then solved numerically. The resultant conductivities are very close to the less extensive results obtained with the higher approximations on the Chapman-Cowling method, provided the Debye shielding distance is used as the cutoff in summing the effects of two-body encounters.

 $\sigma = \frac{2mC^3}{e^2 Z \ln(qC^2)} \left(\frac{2}{3\pi}\right)^{\frac{3}{2}} \gamma_E,$

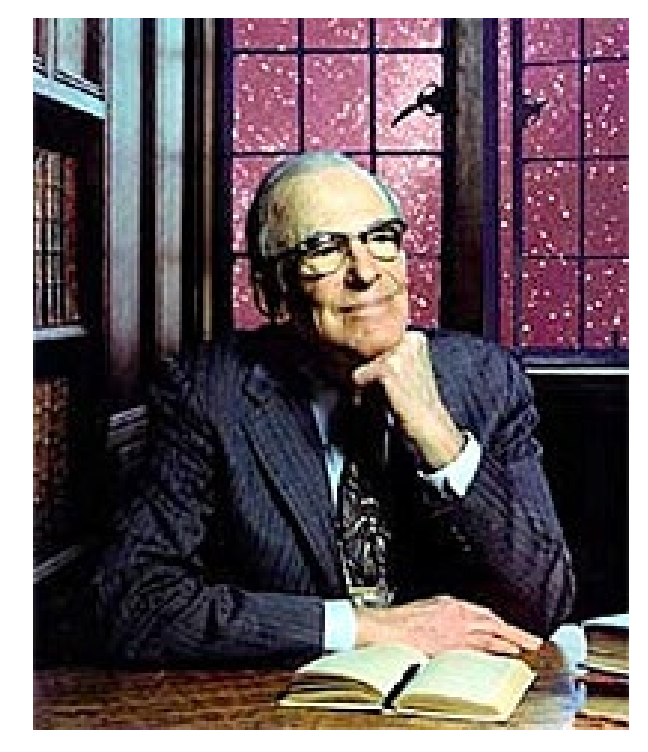
$$\alpha = \frac{3mkC^3}{e^3Z \ln(qC^2)} \left(\frac{2}{3\pi}\right)^{\frac{3}{2}} \gamma_T,$$

$$\beta = \frac{8m^2C^5}{3e^3Z \ln(qC^2)} \left(\frac{2}{3\pi}\right)^{\frac{3}{2}} \delta_E,$$

$$K = \frac{20m^2kC^5}{3e^4Z\ln(qC^2)} \left(\frac{2}{3\pi}\right)^{\frac{3}{2}} \delta_T.$$

TABLE III. Values of transport coefficients.

Z = 1	Z = 2	Z = 4	Z = 16	$Z = \infty$
0.5816	0.6833	0.7849	0.9225	1.000 1.000
0.4652	0.5787	0.7043	0.8870	1.000
$0.2252 \\ 0.4189$	$0.3563 \\ 0.4100$	$0.5133 \\ 0.4007$	0.7907 0.3959	$\frac{1.000}{0.4000}$
	0.5816 0.2727 0.4652 0.2252	0.5816 0.6833 0.2727 0.4137 0.4652 0.5787 0.2252 0.3563	0.5816 0.6833 0.7849 0.2727 0.4137 0.5714 0.4652 0.5787 0.7043 0.2252 0.3563 0.5133	0.5816 0.6833 0.7849 0.9225 0.2727 0.4137 0.5714 0.8279 0.4652 0.5787 0.7043 0.8870 0.2252 0.3563 0.5133 0.7907



26.06.1914-31.03.1997



Conductivity model based on the relaxation time approximation

Y.T. Lee & R.M. More, Physics of Fluids 27, 1273 (1984), more than 750 citations

Lee-More conductivity model based on the RTA is prevalent in applications. Improved by Desjarlais [Contrib. Plasma Phys. **41**, 267 (2001)] to account for partial ionization. However, huge deviations to DFT-MD data occur in the WDM region [French et al., PRE **105**, 065204 (2022)].

An electron conductivity model for dense plasmas

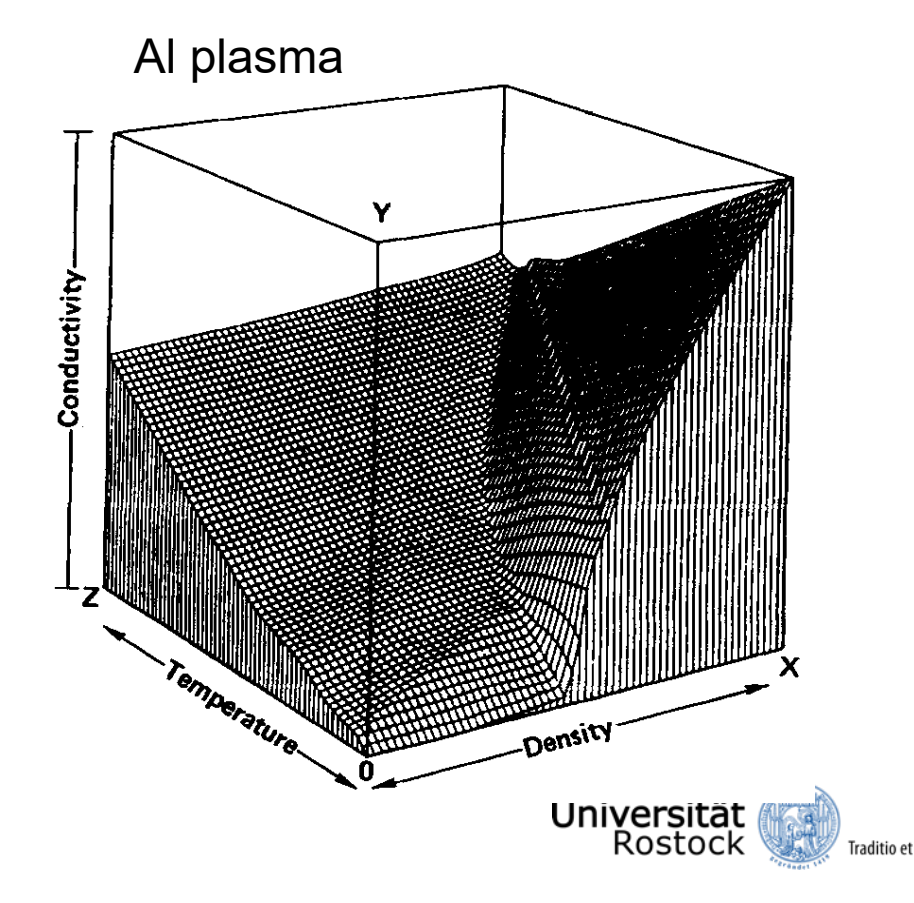
Y. T. Lee and R. M. More

University of California, Lawrence Livermore National Laboratory, Livermore, California 94550

(Received 5 July 1983; accepted 12 December 1983)

An electron conductivity model for dense plasmas is described which gives a consistent and complete set of transport coefficients including not only electrical conductivity and thermal conductivity, but also thermoelectric power, and Hall, Nernst, Ettinghausen, and Leduc-Righi coefficients. The model is useful for simulating plasma experiments with strong magnetic fields. The coefficients apply over a wide range of plasma temperature and density and are expressed in a computationally simple form. Different formulas are used for the electron relaxation time in plasma, liquid, and solid phases. Comparisons with recent calculations and available experimental measurement show the model gives results which are sufficiently accurate for many practical applications.

Alternative conductivity models, e.g., correlation function approach for $S_{ii}(k,\omega)$ and $\epsilon(k,\omega)$ based on the Ziman formula: S. Ichimaru & S. Tanaka, PRA **32**, 1790 (1985)



Composition and transport properties of dense plasmas

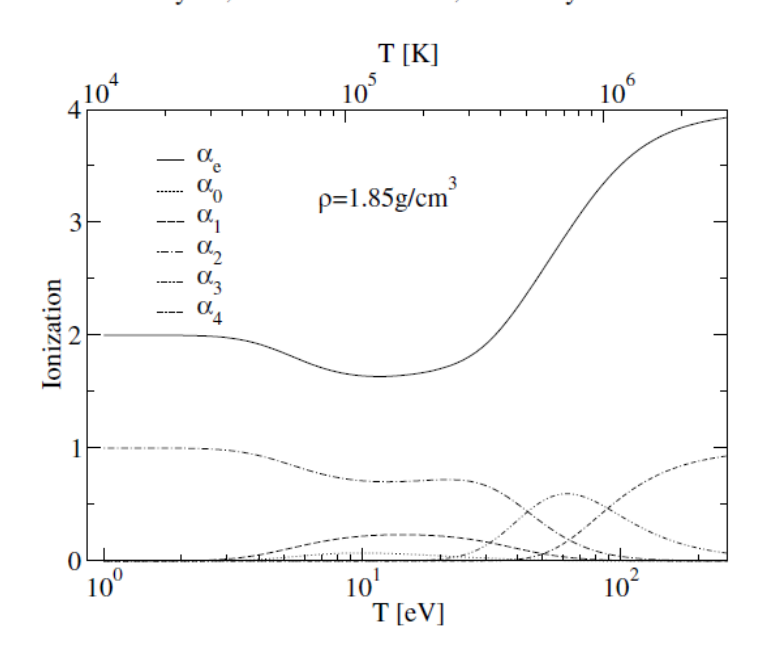
S. Kuhlbrodt, B. Holst & R. Redmer, Contrib. Plasma Physics 45, 73 (2005)

Partially ionized plasma model considering nonideality corrections between all species [beyond Saha eq.]. Linear response theory for the transport coefficients based on Zubarev's approach (1970) [generalized Kubo]. Applicable for dense plasmas but of limited validity in the WDM region [bound states?].

COMPTRA04 – a Program Package to Calculate Composition and Transport Coefficients in Dense Plasmas

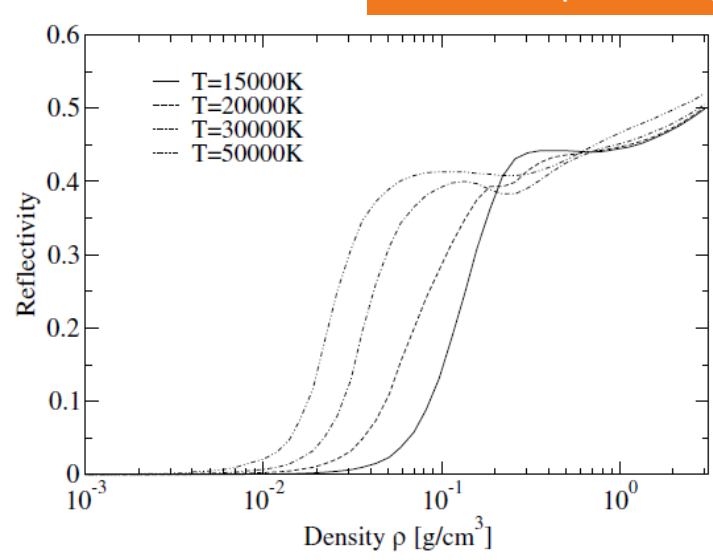
S. Kuhlbrodt, B. Holst, and R. Redmer*

Universität Rostock, Institut für Physik, D-18051 Rostock, Germany



Test case: Be plasma
Applied to metal and noble gas plasmas
S. Kuhlbrodt et al. PRE (2000)
J. Adams et al. PRE (2007)

WD atmospheres? (Talk M. Berrens)

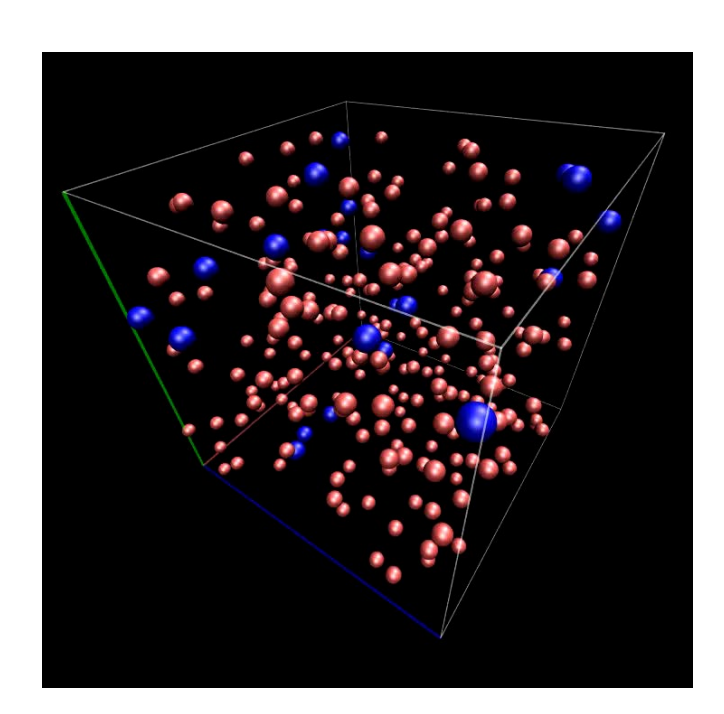




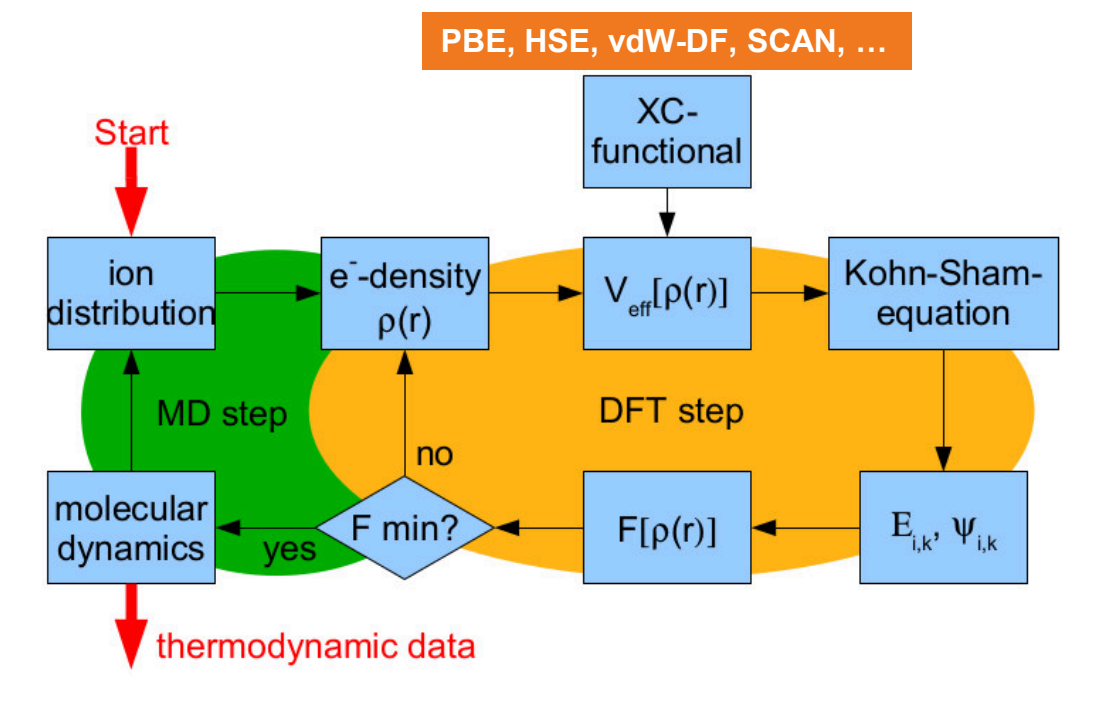
Ab initio data from DFT-MD simulations for WDM & HDM

Vienna Ab-Initio Simulation Package (VASP), Abinit, Quantum Espresso, sDFT ...

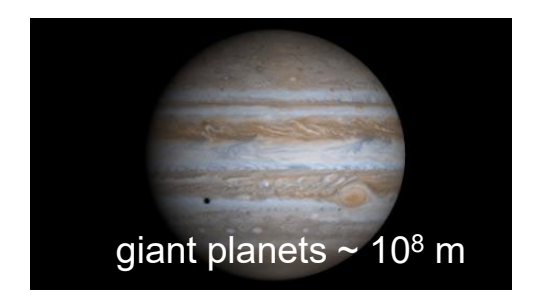
- G. Kresse and J. Hafner, PRB 47, 558 (1993), ibid. 49, 14251 (1994)
- G. Kresse and J. Furthmüller, Comput. Mat. Sci. 6, 15 (1996), PRB 54, 11169 (1996)



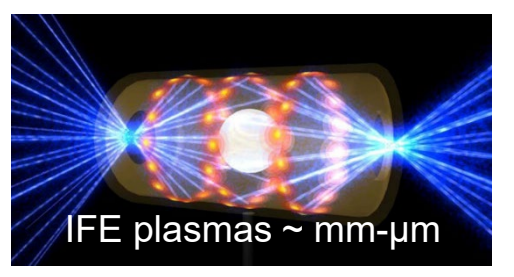




high-pressure phase diagram pair correlation functions electrical & thermal conductivity diffusion coefficient viscosity, opacity









Kubo-Greenwood formula

S. Mazevet et al., HEDP **6**, 84 (2010) B. Holst, M. French, R. Redmer, PRB **83**, 2 35120 (2011)

D.V. Knyazev, P.R. Levashov, Comp. Mat. Sci. 79, 817 (2013)

Currents and Onsager coefficients: σ

$$\langle \mathbf{J}_{e} \rangle = \frac{1}{q} \left(q L_{11} \mathbf{E} + \frac{L_{12} \nabla T}{T} \right) \qquad \sigma = \lim_{\omega \to 0} L_{11}(\omega),$$

$$\langle \mathbf{J}_{q} \rangle = \frac{1}{q} \left(q L_{21} \mathbf{E} + \frac{L_{22} \nabla T}{T} \right) \qquad \lambda = \lim_{\omega \to 0} \frac{1}{T} \left(L_{22}(\omega) - \frac{L_{12}^{2}(\omega)}{L_{11}(\omega)} \right)$$

Onsager coefficients L_{mn} via Kubo-Greenwood formula:

$$L_{mn}(\omega) = \frac{2\pi q^{4-m-n}}{3Vm_e^2 \omega} \sum_{\mathbf{k}\nu\mu} |\langle \mathbf{k}\nu|\hat{\mathbf{p}}|\mathbf{k}\mu\rangle|^2 (f_{\mathbf{k}\nu} - f_{\mathbf{k}\mu})$$

$$\times \left(\frac{E_{\mathbf{k}\mu} + E_{\mathbf{k}\nu}}{2} - h_e\right)^{m+n-2} \delta(E_{\mathbf{k}\mu} - E_{\mathbf{k}\nu} - \hbar\omega)$$

Evaluation by using DFT-MD data (Kohn-Sham orbitals and energies)



High pressure phase diagram of dense liquid hydrogen

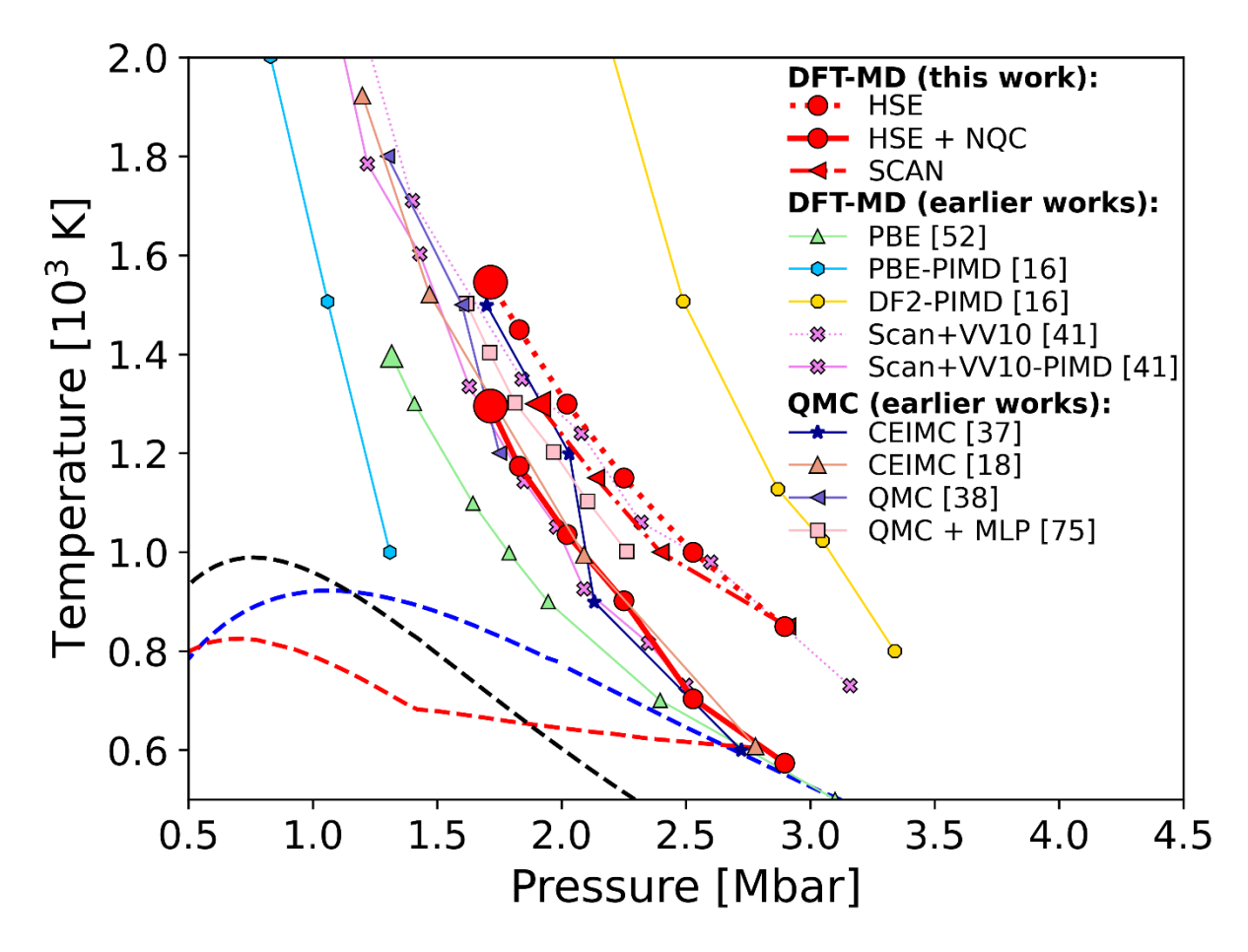
1st-order liquid-liquid phase transition: NVT ensemble with 512 atoms, various XC functionals

TABLE I. Comparison of input parameters for DFT-MD simulations between this and earlier works. Compared are the XC functional, the number of atoms *N*, the **k**-point set used to evaluate the Brillouin zone (BZ), and simulation length (SL).

References	XC functional	N	BZ	SL (ps)
Lorenzen et al. ²⁴	PBE	512	BP	<10
Geng et al. ²⁵	PBE+revPBE-DF	3456	BP	1.5
Morales et al. 16	PBE+DF2	128-432	Γ	1.5 - 2.0
Knudson et al. ³³	DF1 and DF2	265	BP	Few ps
Hinz et al.41	SCAN-rVV10	256	Γ	0.5-0.6
van de Bund <i>et al.</i> ⁴⁴	BLYP	360	BP	1
Tian et al. ⁴⁵	PBE	64	$3 \times 3 \times 3$	2
Lu et al. ⁴⁸	PBE0-rVV10 + rVV10 + DF1	256	Γ	2-5
Present	HSE	512	BP	3-12

TABLE II. Comparison of critical points obtained by using different XC functionals.

References	XC functional	p (Mbar)	<i>T</i> (K)	
Lorenzen et al. ²⁴	PBE	1.32	1400	
This work	SCAN	1.91	1300	
This work	HSE	1.71	1550	
This work	HSE+NQE	1.71	1296	





High pressure phase diagram of dense liquid hydrogen

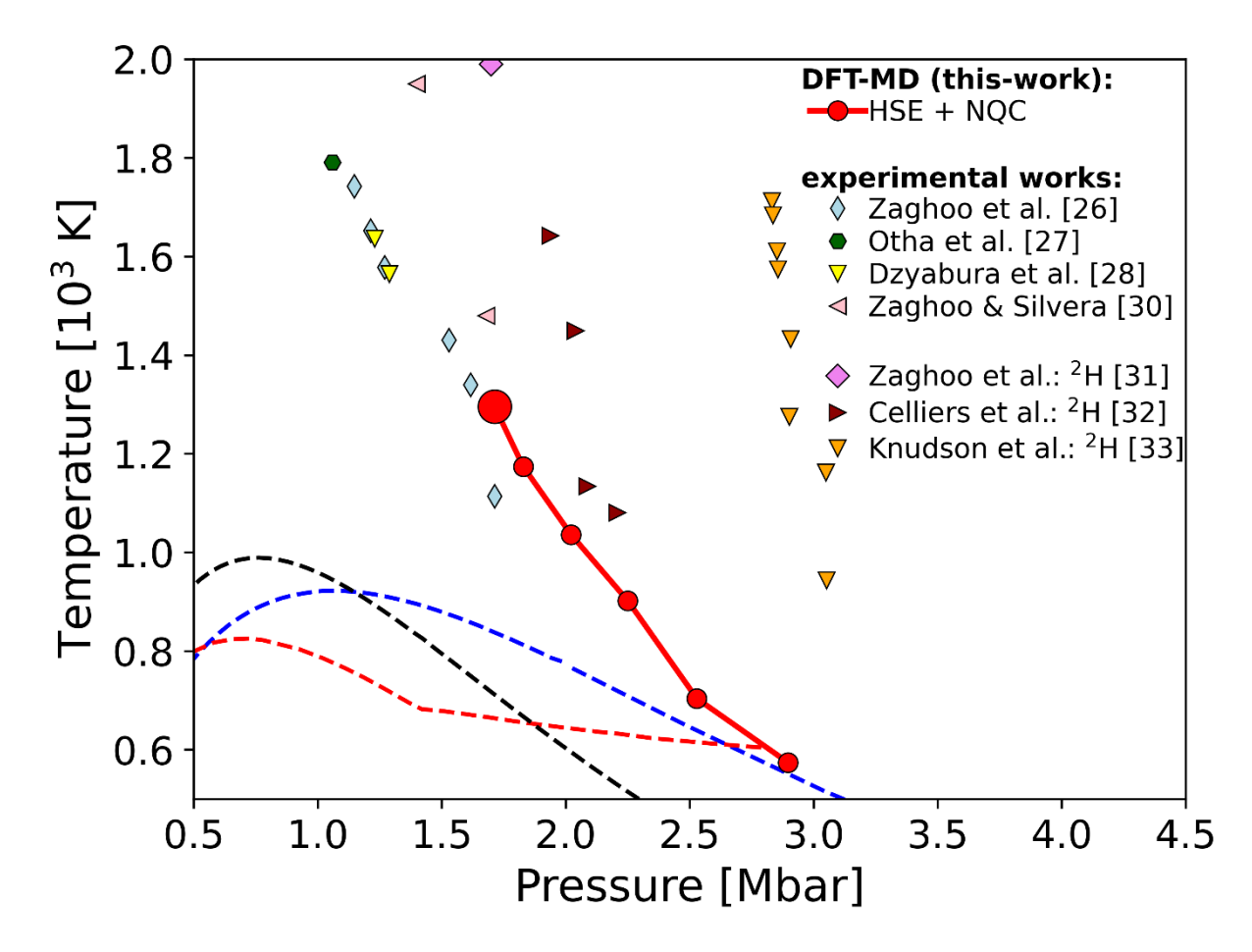
1st-order liquid-liquid phase transition: comparison with experiments

TABLE I. Comparison of input parameters for DFT-MD simulations between this and earlier works. Compared are the XC functional, the number of atoms *N*, the **k**-point set used to evaluate the Brillouin zone (BZ), and simulation length (SL).

References	XC functional	N	BZ	SL (ps)
Lorenzen et al. ²⁴	PBE	512	BP	<10
Geng et al. ²⁵	PBE+revPBE-DF	3456	BP	1.5
Morales et al. ¹⁶	PBE+DF2	128-432	Γ	1.5 - 2.0
Knudson et al. ³³	DF1 and DF2	265	BP	Few ps
Hinz et al. ⁴¹	SCAN-rVV10	256	Γ	0.5-0.6
van de Bund <i>et al.</i> ⁴⁴	BLYP	360	BP	1
Tian et al. ⁴⁵	PBE	64	$3 \times 3 \times 3$	2
Lu et al. ⁴⁸	PBE0-rVV10 + rVV10 + DF1	256	Γ	2-5
Present	HSE	512	BP	3-12

TABLE II. Comparison of critical points obtained by using different XC functionals.

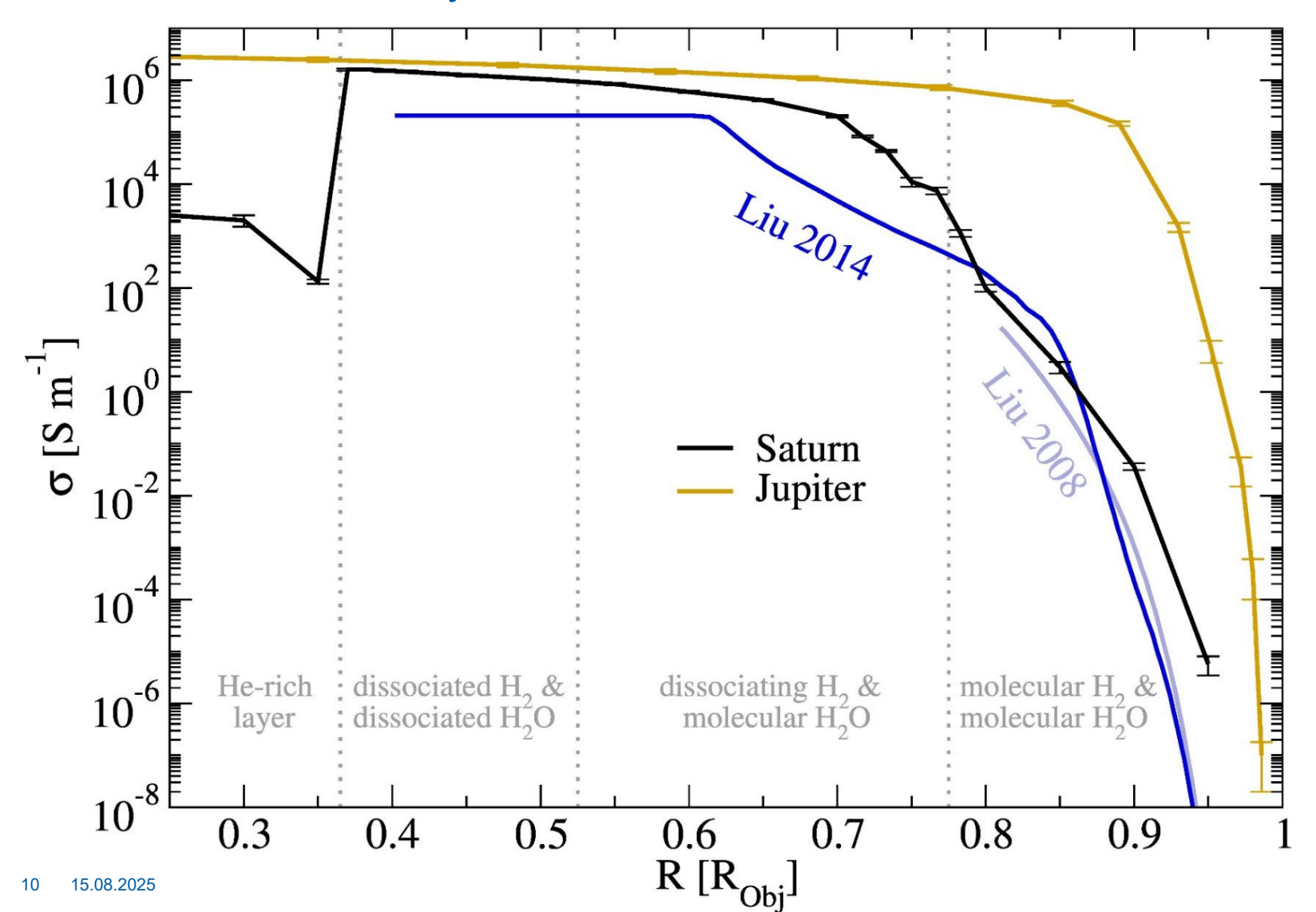
References	XC functional	p (Mbar)	<i>T</i> (K)	
Lorenzen et al. ²⁴	PBE	1.32	1400	
This work	SCAN	1.91	1300	
This work	HSE	1.71	1550	
This work	HSE+NQE	1.71	1296	





Material properties in Saturn

Electrical conductivity



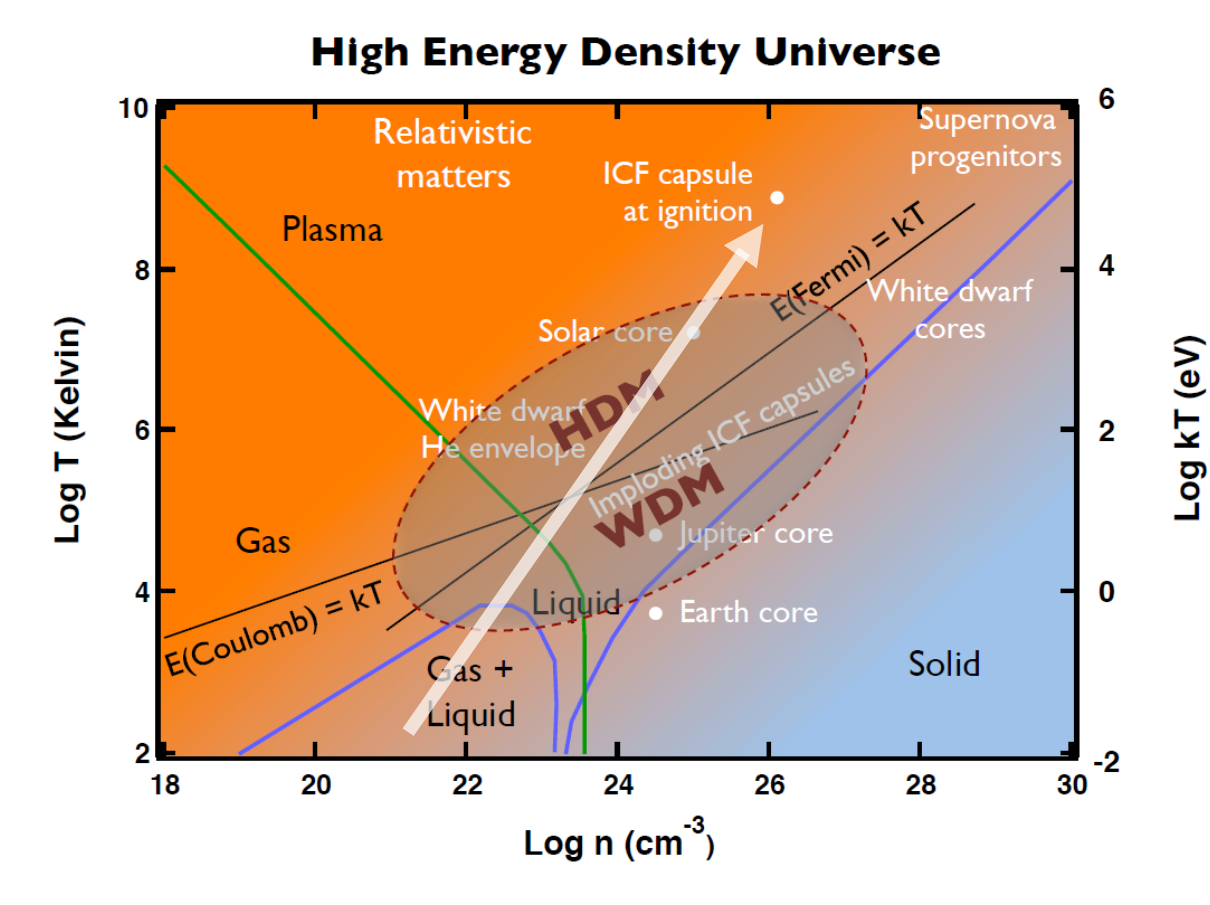
Input into dynamo simulations: B field

Saturn: M. Preising et al., ApJS **269**, 47 (2023) Jupiter: M. French et al., ApJS **202**, 5 (2012)

Using the HSE XC functional (reliable band gaps)

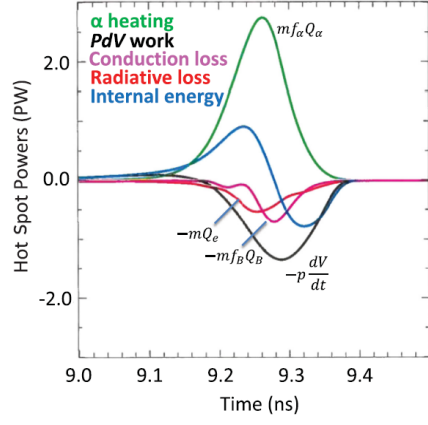


Plasmas for IFE cover warm & hot dense matter



See: Basic Research Needs for High Energy Density Laboratory Physics (DOE Office of Science and NNSA, 2010) To reliably **predict and control** the path of compression experiments from a cold initial state through WDM to a burning plasma, accurate data for the **microphysics**, e.g.,

- nuclear reaction rates
- stopping power
- EOS
- transport coefficients
- opacity are needed for
- a wide range of P-T-p
- target and support materials
- which are usually mixtures.



H. Abu-Shawared et al., PRL **129**, 075001 (2022) (Talk A. Kritcher)

- → input in **PIC** and **rad-hydro** simulations
- → mandatory to analyze **flagship** experiments
- → on the way to an **IFE power plant**



U. Kleinschmidt & R. Redmer, Matter Rad. Extrem. 10, 057602 (2025)

Goal: Provide an improved LM model based on DFT-MD data for a wide range of P-T-ρ conditions, keeping the analytical simplicity of the LM model and covering fully and partially ionized hydrogen plasma

 $\rho = (0.1 - 8) \text{ g/cm}^3 \text{ and } T = (2000 - 500 000) \text{ K}$

Onsager coefficients:

$$K_n = -\frac{2m_e}{3\pi^2\hbar^3} \int_0^{\infty} dE \, \frac{E^{n+1}}{\sum_s n_s Q_{es}(E)} \frac{\partial f_e^0}{\partial E},$$

Conductivities:

$$\sigma_e = e^2 K_0, \qquad \lambda_e = \frac{1}{T} \left(K_2 - \frac{K_1^2}{K_0} \right).$$

Electron-ion contribution:

(e-e and e-neutral as well)

$$K_{n,eI} = -\frac{2^{3/2} m_e^{1/2} P(T,\rho_I)}{3\pi^2 \hbar^3 n_I Z_I^2} \int_0^{\infty} dE \ E^{n+3} \frac{\partial f_e^0}{\partial E}.$$

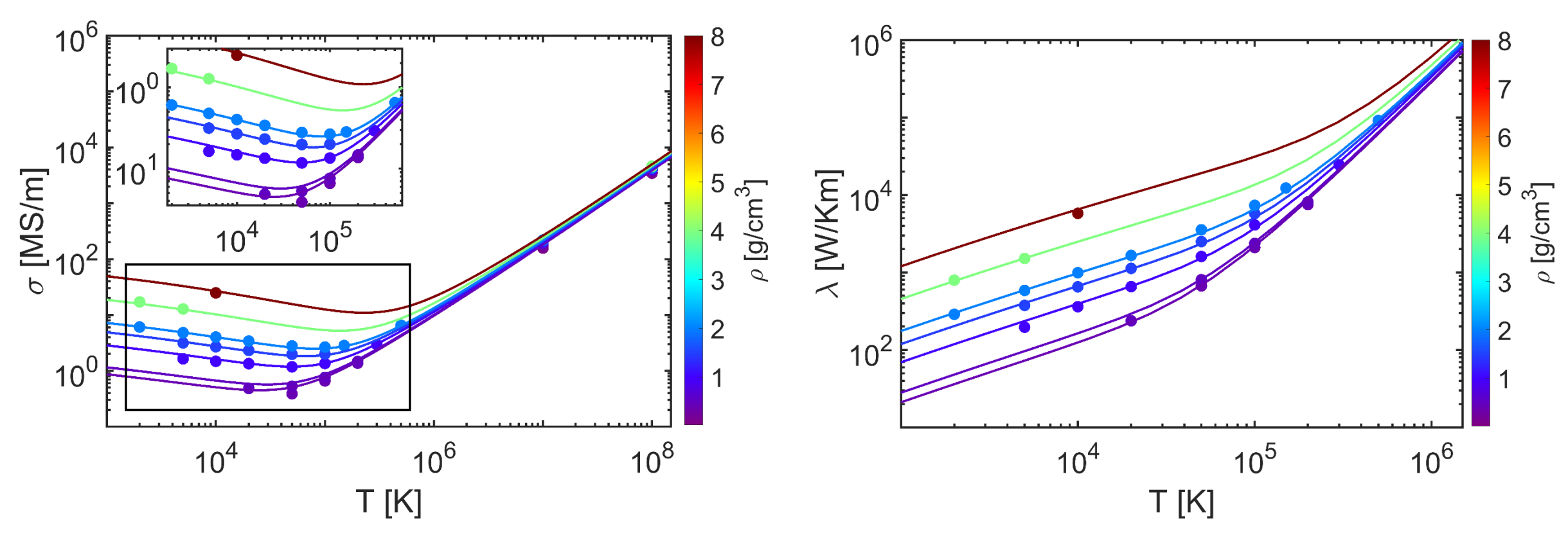
Fit function based on the DFT-MD data instead of the values from the RTA: (parameters given in the paper)

$$\begin{split} P(T,\rho_I) &= a_0 T^{a_1} \rho^{a_2} + a_3 \rho^{a_4} + a_5 \\ &+ a_6 \rho^{a_7} \, \exp \left[- \left(\frac{\log T - a_8}{a_9} \right)^2 \right], \end{split}$$



U. Kleinschmidt & R. Redmer, Matter Rad. Extrem. 10, 057602 (2025)

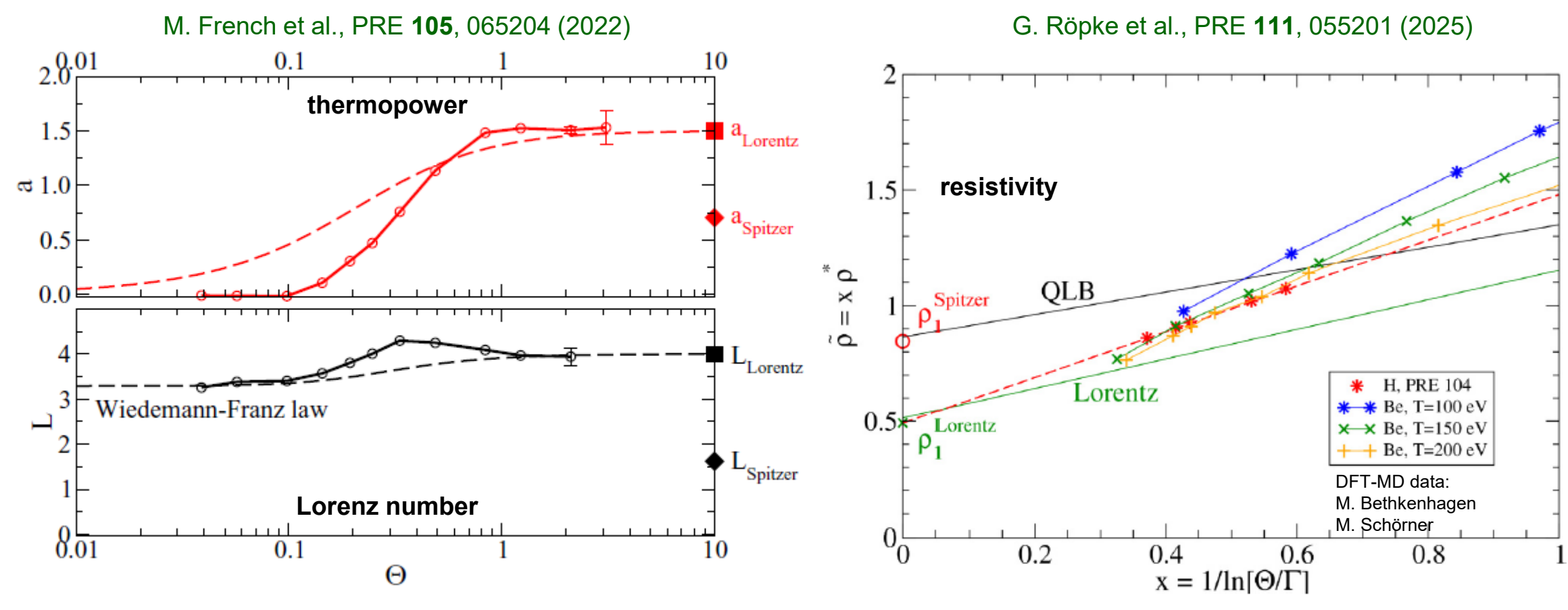
Goal: Provide an improved LM model based on DFT-MD data for a wide range of P-T-p conditions, keeping the analytical simplicity of the LM model and covering **fully ionized** hydrogen plasma





Classical limit: Spitzer theory (e-i & e-e) vs. Lorentz gas model (e-i)

Electron-electron scattering captured in DFT? Computational challenge!



Study H across the plasma plane along $\Gamma^8\Theta^7=1$



 $\Gamma = (Ze)^2/4\pi\epsilon_0 k_B Td$

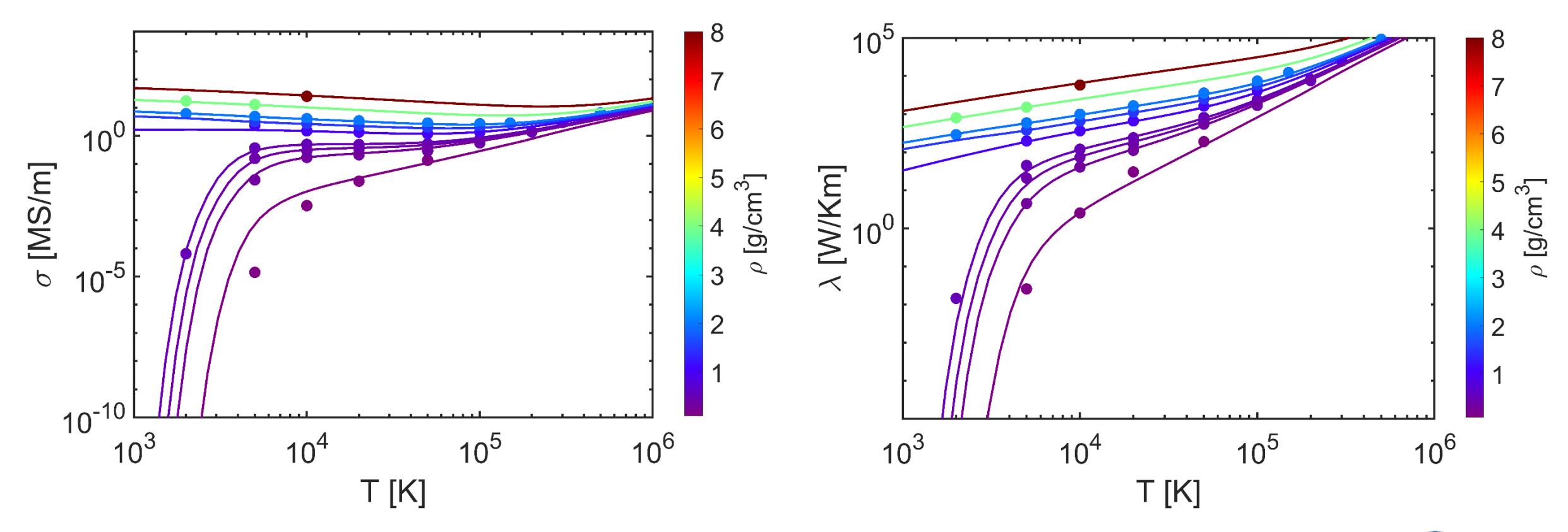
Perform a virial expansion

$$\frac{\Theta}{\Gamma} = \frac{2}{(12\pi^5)^{1/3}} \frac{T_{\text{Ha}}^2}{n_{\text{Boh}}}$$



U. Kleinschmidt & R. Redmer, Matter Rad. Extrem. 10, 057602 (2025)

Goal: Provide an improved LM model based on DFT-MD data for a wide range of P-T-p conditions, keeping the analytical simplicity of the LM model and covering **partially ionized** hydrogen plasma

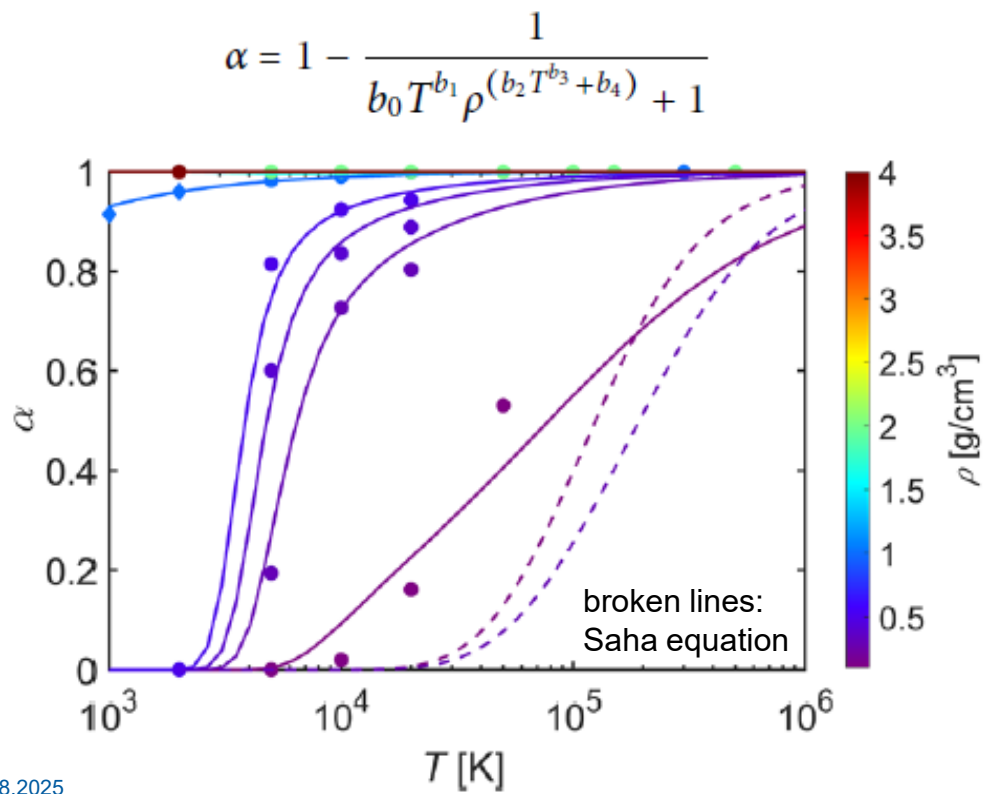


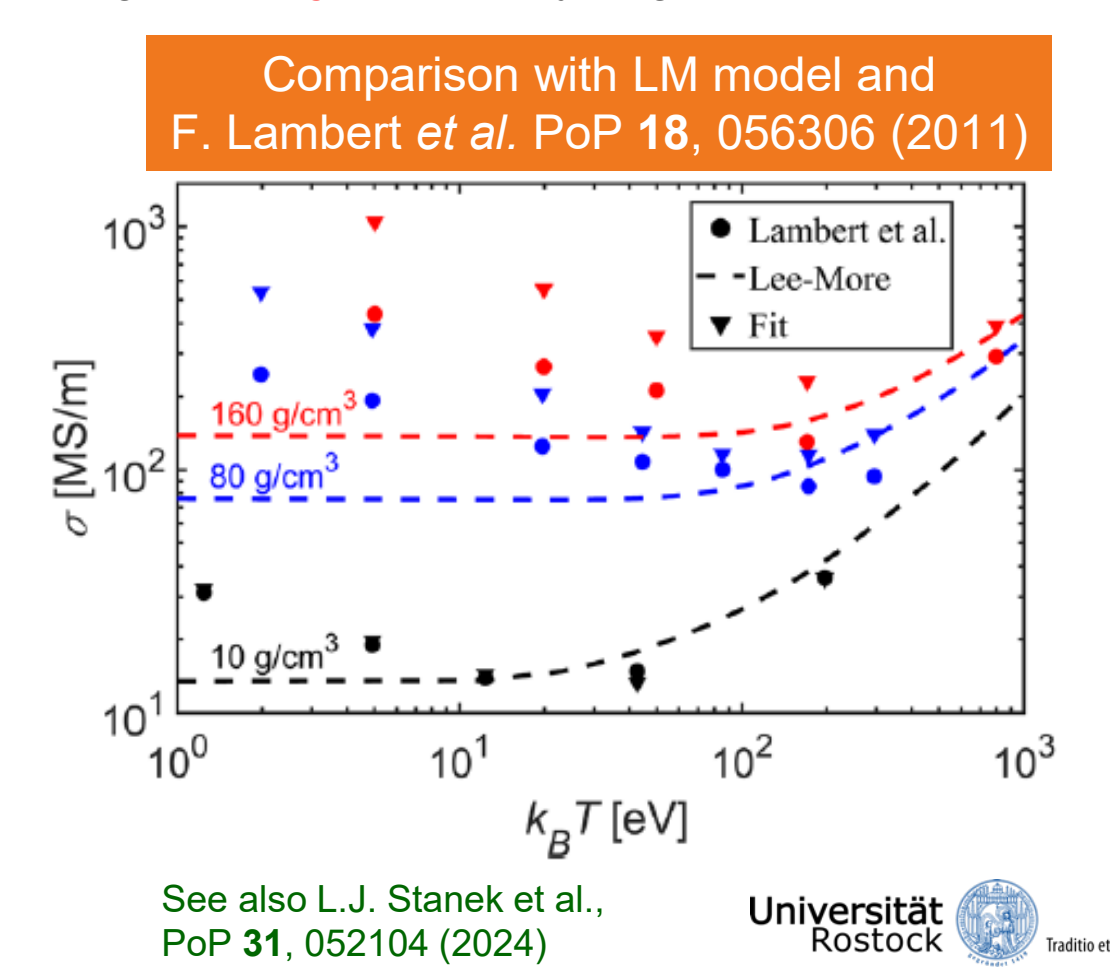


U. Kleinschmidt & R. Redmer, Matter Rad. Extrem. 10, 057602 (2025)

Goal: Provide an improved LM model based on DFT-MD data for a wide range of P-T-p conditions, keeping the analytical simplicity of the LM model and covering partially ionized hydrogen plasma

Fit formula for the ionization degree





Conclusions

- Extensive DFT-MD simulations for matter under extreme conditions: WDM & HDM
- Increased computational power available, e.g., N ≥ 512 with HSE XC functional for H
- Provide EOS data and conductivities for a wide range of P-T-ρ conditions
- Input for hydro and rad-hydro simulations for WDM & HDM
- Impact on state-of-the-art planetary models (interior, evolution, B field)
- New concepts for IFE towards a fusion power plant
- Design and analyze flagship experiments using HPL and brilliant X-ray sources (FELs)
- Fusion 2040 Program of the BMFTR (Marvel Fusion, HZDR, European XFEL, UR, CALA)
- Provide ab initio data for the microphysics for corresponding materials and plasma parameters

12th Joint Workshop on High Pressure, Planetary and Plasma Physics (12HP4) 22-24 Sep 2025 at European XFEL in Schenefeld, Germany



Acknowledgments

Armin Bergermann (SLAC) Mandy Bethkenhagen (LULI) **Thomas Bornath Martin French (Fraunhofer) Uwe Kleinschmidt** Anna Julia Poser (FUB) **Martin Preising Argha Roy (HZDR) Ludwig Scheibe (DLR)** Maximilian Schörner Jan Maik Wissing (DLR)











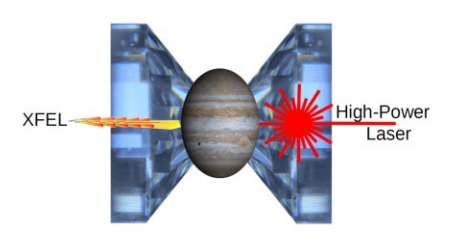












Research Unit FOR 2440 "Matter under Planetary Interior Conditions" (2017-2024)



Priority Program SPP 1992 "The Diversity of Exoplanets" (2017-2023)









